Smart Structures and Systems, *Vol. 33*, *No. 4* (*2024*) *313-323*
https://doi.org/10.12989/sss.2024.33.4.313

A deep neural network to automatically calculate the safety grade of a deteriorating building

Seungho Kim [1a], Jae-Min Lee [2b], Moonyoung Choi [2c] and Sangyong Kim*[2]

[1] *Department of Architecture*, *Yeungnam University College*, *170 Hyeonchung-ro*, *Nam-gu*, *Daegu 42415*, *Republic of Korea*
[2] *School of Architecture*, *Yeungnam University*, *280 Daehak-ro Gyeongsan-si*, *Gyeongsangbuk-do 38541*, *Republic of Korea*

(*Received May 20*, *2022 Revised October 12*, *2023*, *Accepted April 26*, *2024*)

Abstract. Deterioration of buildings is one of the biggest problems in modern society, and the importance of a safety diagnosis for old buildings is increasing. Therefore, most countries have legal maintenance and safety diagnosis regulations. However, the reliability of the existing safety diagnostic processes is reduced because they involve subjective judgments in the data collection. In addition, unstructured tasks increase rework rates, which are time-consuming and not cost-effective. Therefore, This paper proposed the method that can calculate the safety grade of deterioration automatically. For this, a DNN structure is generated by using existing precision inspection data and precision safety diagnostic data, and an objective building safety grade is calculated by applying status evaluation data obtained with a UAV, a laser scanner, and reverse engineering 3D models. This automated process is applied to 20 old buildings, taking about 40% less time than needed for a safety diagnosis from the existing manual operation based on the same building area. Subsequently, this study compares the resulting value for the safety grade with the already existing value to verify the accuracy of the grade calculation process, constructing the DNN with high accuracy at about 90%. This is expected to improve the reliability of aging buildings in the future, saving money and time compared to existing technologies, improving economic efficiency.

Keywords: field measurement; infrastructure maintenance; nondestructive evaluation; smart system; smart technology; structural health monitoring

1. Introduction

Over the past few decades, the number of deteriorated buildings has increased, and maintenance and safety diagnoses of such buildings have been recognized as very important long-term problems in the life cycle of buildings (Kwon *et al*. 2020). Therefore, the importance of safety diagnosis and maintenance measures for deteriorated buildings is increasing. Currently, most countries conduct building appearance surveys and safety diagnoses based on detailed guidelines and evaluation criteria (Anuar *et al*. 2019). However, an evaluation method based on detailed guidelines makes it difficult to obtain objective data (Park *et al*. 2016, Liu *et al*. 2019). In other words, because the process is not uniform, it takes time to complete, which reduces the objectivity of the data, resulting in a cost increase (Ensafi and Thabet 2021). Park and Kim (2020) noted that as the main body of building safety diagnosis shifts from public to private, efficient and objective research into a uniform structural safety diagnosis is needed. In addition, since the bidding process is to submit the lowest price during selection of private companies, the differences in the levels and perspectives of individual experts may affect the results, and reduce objectivity (Park *et al*. 2017). Therefore, Shi and Ergan (2020) said, the work process should be divided up and standardized methods and report forms should be presented. It was confirmed that the data collection method for existing deteriorated buildings has limitations in objectivity and does not represent a typical process. The term safety grade refers to comprehensive calculation of data results from an actual safety diagnosis based on visual and safety inspections of deteriorated buildings (Park *et al*. 2016). There are two types of problem with this deteriorated building safety diagnosis process. The first is to select private companies based on the lowest bid, and that one or more companies will conduct building safety management. This is difficult to express politically because information is collected manually, and the results may vary depending on the individual's level of expertise and personal perspectives. In the end, the reliability of the results may become a problem. A second form of the report is submitted after the external inspection and safety diagnostic processes. Reports submitted after the appearance investigation and safety diagnosis vary from time to time (Shi and Ergan 2020). This is not only because existing data cannot be used in future safety diagnoses, but they also take a lot of time to complete. In addition, objectivity may be reduced by increasing costs and increasing the amount of data returned. Therefore, objectivity and formulation of new processes are

*Corresponding author, Professor,
E-mail: sangyong@yu.ac.kr
[a] Professor, E-mail: kimseungho@ync.ac.kr
[b] M.S., E-mail: jerry0719@ynu.ac.kr
[c] Ph.D. Student, E-mail: cmy841@ynu.ac.kr

ISSN: 1738-1584 (Print), 1738-1991 (Online)

necessary to solve existing shortcomings.

Recently, many studies have been conducted on the appearance of aging buildings by using high-precision measuring equipment (Kang *et al*. 2016, Choi *et al*. 2018, Falorca and Lanzinha 2020, Pan *et al*. 2020, Wu *et al*. 2023). However, most studies do not cover the safety of buildings. In addition, existing studies have conducted condition evaluations based on building appearance surveys, excluding considerations for building safety, and making it difficult to calculate comprehensive building safety grades.

To address this limitation, this paper proposes an automated grade calculation using 3D point clouds. In the first step, a DNN structure was generated based on existing safety diagnosis process of deteriorated buildings. In the second step, building condition data acquired by high-precision measuring devices was applied to DNN.

2. Review of previous building deterioration assessment

2.1 Safety diagnostics using high-precision measuring devices

Visual inspection is one of the basic methods of exterior inspection to measure risk factors visually or by using measuring devices according to detailed guidelines and evaluation criteria tables (Kwan and Ng 2015, Anuar *et al*. 2019). A visual inspection entails the subjective nature of experts or examiners (Park *et al*. 2016, Guo and Wang 2022). Also, exterior inspection results are less objective because they depend on the level of expertise and the perspective of the individual (Park *et al*. 2017). For this reason, existing studies presented objectivity and reliability problems with visual inspection data (Liu *et al*. 2019). With recent developments in devices, more studies have been conducted on exterior inspections using unmanned aerial vehicles (UAVs) and laser scanners to analyze the condition of buildings (Rachmawati and Kim 2022). Falorca and Lanzinha (2020) identified the performance levels of buildings and proposed maintenance measures by acquiring data through exterior inspections using UAVs and analyzing preservation status based on the External Thermal Insulation Composite System. In addition, research is underway to combine technologies such as forward-looking infrared (FILR) and virtual reality (VR) with UAVs to present a process for visually determining building conditions (Liu *et al*. 2019, Pan *et al*. 2020).

Laser scanning technology is used to accurately record the current structure of a building (Kwon 2009, Chen *et al*. 2022, Klapa 2023). Three-dimensional point cloud and stereo images acquired with a laser scanner have been studied over the past decade for crack detection and measurement. Law *et al*. (2015) confirmed that laser scanning technology provides objective and precise data for exterior inspection and surface deterioration of buildings. Based on proven facts, Turkan *et al*. (2018) analyzed 3D point cloud data to examine the damaged area of a tunnel. In addition, studies were also conducted to identify cracks in damaged areas of large-scale structures, such as bridges and dams (Lattanzi and Miller 2014, Mukupa *et al*. 2016). This proved that cracks of at least 2 mm or more can be detected, and the average error was about 2~3 mm (Vasić *et al*. 2014, Ani *et al*. 2015, Sarker *et al*. 2017).

However, since the results of existing studies are derived manually, rather than automatically, subjective opinions of experts may be reflected in the data. The process presented in previous studies is not automatic but passive, so it is time-consuming and not cost-effective to evaluate the condition of many buildings. In addition, evaluation of the durability and safety of buildings is excluded because only appearance surveys are used to distinguish condition grades, and comprehensive safety grades are difficult to calculate.

2.2 Safety diagnostic using machine learning

Deep learning is an inverted model of the artificial neural network (ANN) that consists of layers in the ANN (Marcus 2018). Due to technological constraints, early research was conducted through relatively simple neural networks, such as the ANN. Silva *et al*. (2013) tried to measure the durability of buildings based on statistical perspective linear regression and an ANN to produce mathematical models to calculate appearance grades. Sousa *et al*. (2014) used a support vector machine (SVM) and an ANN to predict the state of a structure and compare the results, presenting their advantages. El-Abbasy *et al*. (2014) also predicted the state of the ANN pipeline, raising the problem that simple neural networks are less accurate than complex neural networks, such as the deep neural network (DNN) and the convolutional neural network (CNN).

With recent developments in computer hardware, crack detection studies using the CNN and the DNN (types of deep learning algorithms) have been carried out. The majority of research is based on defect images (Nex *et al*. 2019, Luo *et al*. 2019, Zhang *et al*. 2023, Chaiyasarn *et al*. 2022). Cha *et al*. (2017) confirmed that 98% accuracy can be obtained by understanding crack location and size information through algorithmic models obtained by digitizing the image data obtained. However, since existing research is an algorithmic model limited to only one item called a crack, it is difficult to apply such models to an overall building appearance survey.

Kang and Cha (2018) proposed a new inspection system using ultrasonic beacons, a CNN, and geo-tagging methods to confirm the advantages of global positioning system (GPS) signals in closed environments for structural sensing and positioning. Gopalakrishnan *et al*. (2018) also presented an outline for finding automated defects using UAVs, image data, and deep learning. Perez *et al*. (2019) used a CNN layer to understand crack location information and surface aging information, and then created a confusion matrix based on the learned data to visualize them. Cheng *et al*. (2020) finally integrated building information modeling (BIM) and Internet of Things (IOT) technologies and applied ANN and SVM machine learning algorithms to demonstrate the maintenance and state prediction processes for mechanical, electrical, and plumbing (MEP) components. However, in existing studies, deep learning structures such as the ANN and DNN were used to confirm

only information about appearance damage and locations on buildings, bridges, and MEP components. This is because structural evaluation of the durability and safety of buildings was not carried out, making it difficult to calculate an overall grade.

Therefore, the purpose of this study is to calculate the safety grades of buildings by using objective and reliable state evaluation data and accurate safety diagnosis data obtained after using a UAV and laser scanner. In addition, automatic calculation of the safety grades of aging buildings using deep learning, which improves time- and cost-efficiency, is presented.

3. Automated grade calculation methodology

3.1 Generating deep learning–based building safety grade prediction model

3.1.1 Relocate and modify existing status evaluation data

We utilize existing traditional visual inspection data for creating the deep learning model. The data were divided into textual data, such as Excel and CSV spreadsheets, and binary data such as images and audio. The advantages of textual data are convenience to modify and process them using a simple editor, plus they are inexpensive, and the processing speed is fast. In this study, textual data suitable for DNN learning are used in two data formats that are easy to process and modify. The resulting values of the current visual inspection data are status evaluations of the parts and floors, but status values of the data for each item based on visual inspection are unknown. This only shows the overall condition of the building, and it is unclear which items are the most deteriorated, and which repair and reinforcement earlier into seven items that can be acquired from shape information.

Fig. 1 shows the safety diagnosis data of the deteriorated buildings, merged into seven categories and processed into textual data. The total number of safety diagnostic items for the processed deteriorated buildings is 291, which may include variations due to the differences in the amount of data at each level. In particular, grade E buildings cannot be used due to the structural problems, so it is difficult to acquire grade E building data. If deviations occur, the accuracy of the DNN may be reduced, and the results may vary depending on the randomly selected training, testing, and validation data. Therefore, in order to solve the problems presented in this study, over-sampling was carried out. Data over-sampling refers to generating a small number of new data from the original dataset to reach the required amount of data. In this study, the data over-sampling used R to generate a total of 1,000 pieces of data, 250 each for grades A, B, C, and D.

3.1.2 Deep-learning data analysis

In this study, a deep learning toolbox called nntool was used to teach the DNN through Matlab and another DNN. Input data, output data, and target data were specified as variables that can be imported, and the DNN generated imported data in a space called Networks. The resulting DNN can be learned, and the resulting values can be generated in the output data space to derive the final values. The procedure for deep learning data analysis in this study is in Fig. 2. In order to use data in Matlab, variables for the input layer and target layer must be generated. Variables used in the input layer include input data, which are input values, and target data, which are used to verify the learned model. The output value or output data (that is, the variables for the layer that presents the basis for the resulting values

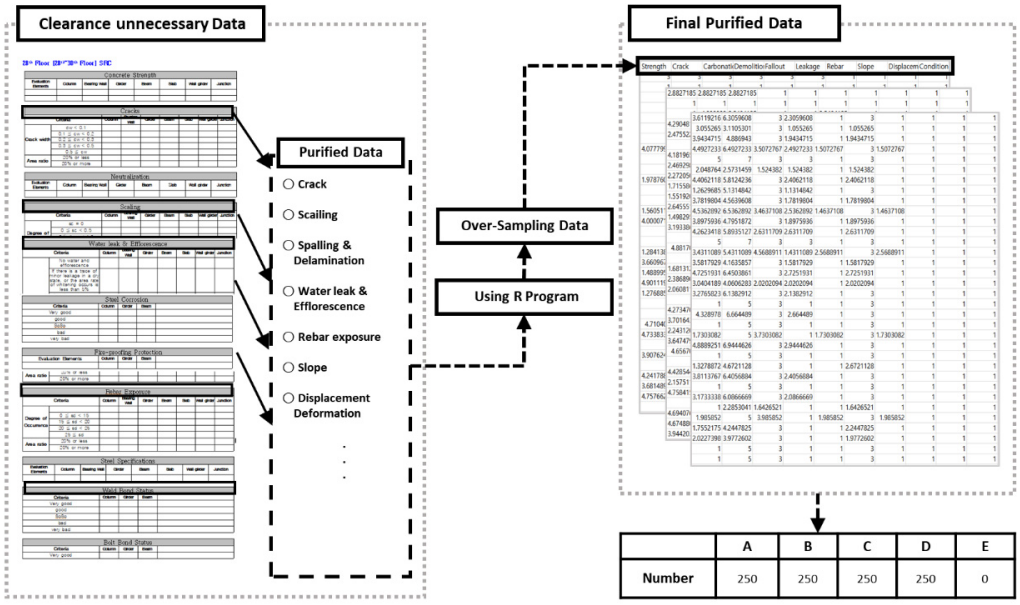

Fig. 1 Acquired condition assessment results

procedures should be prioritized. Therefore, in this study,the data are processed by categorizing the nine items mentioned

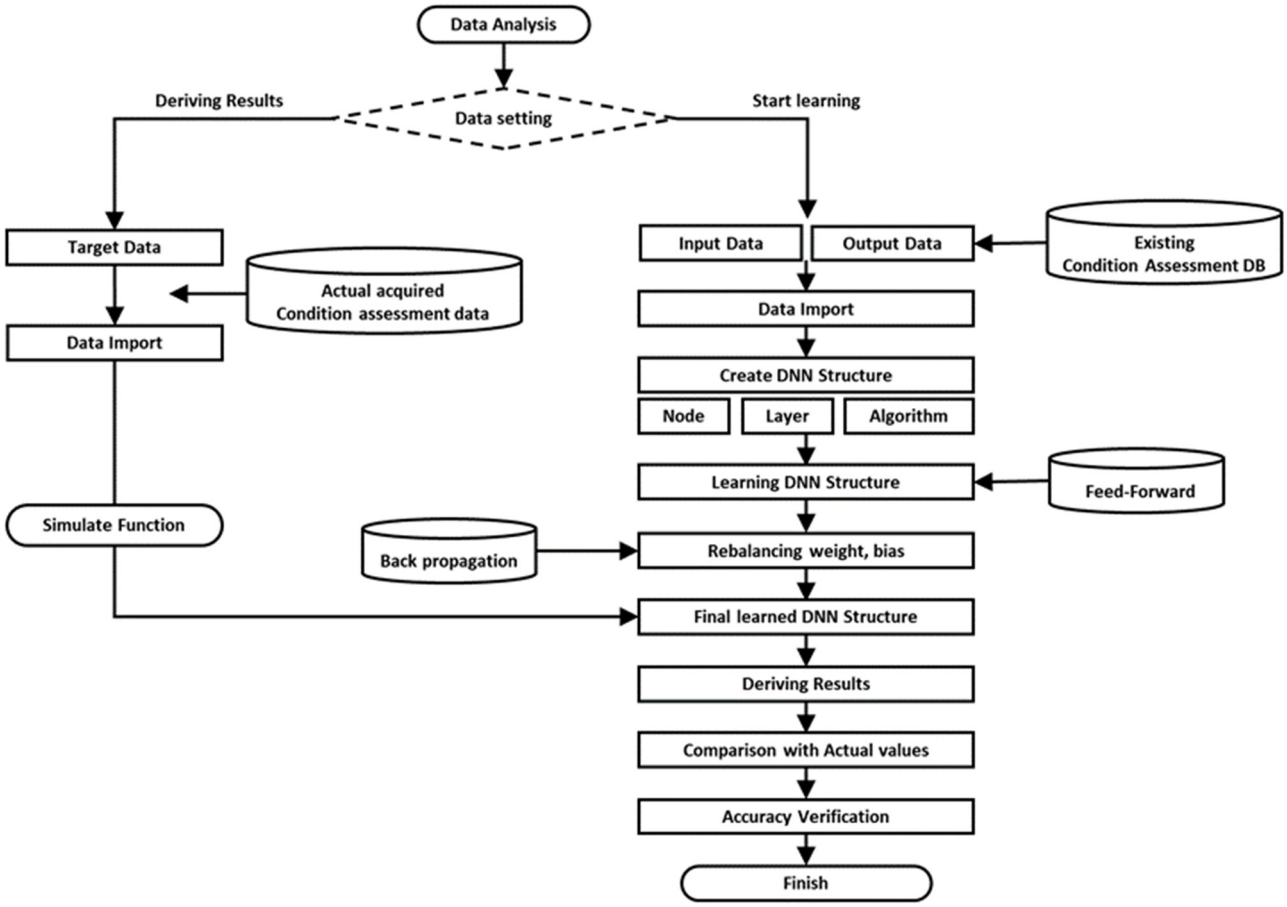

Fig. 2 DNN data analysis process

of the model) are learned through the input data. Each variable must have data, and the process of entering such data is called data setting. Input data, output data, and target data variables must be imported into the appropriate layer through the nntool Neural Network Data Manager. This means that preparation work for the production of DNN structures has been completed. The imported data are selected through the network data manager according to the required network type, the number of hidden layers, the number of nodes in each layer, and the values of the data you want in order to execute the learning process. Each hidden layer is automatically calculated according to the number of nodes set in the first layer for learning. The DNN learns from weighted values, Weight (w), and biased values, Bias (b), and initial data learning is performed with a feed-forward algorithm. After verification using a backpropagation algorithm, the value of w is re-adjusted to generate a DNN structure that can accurately learn.

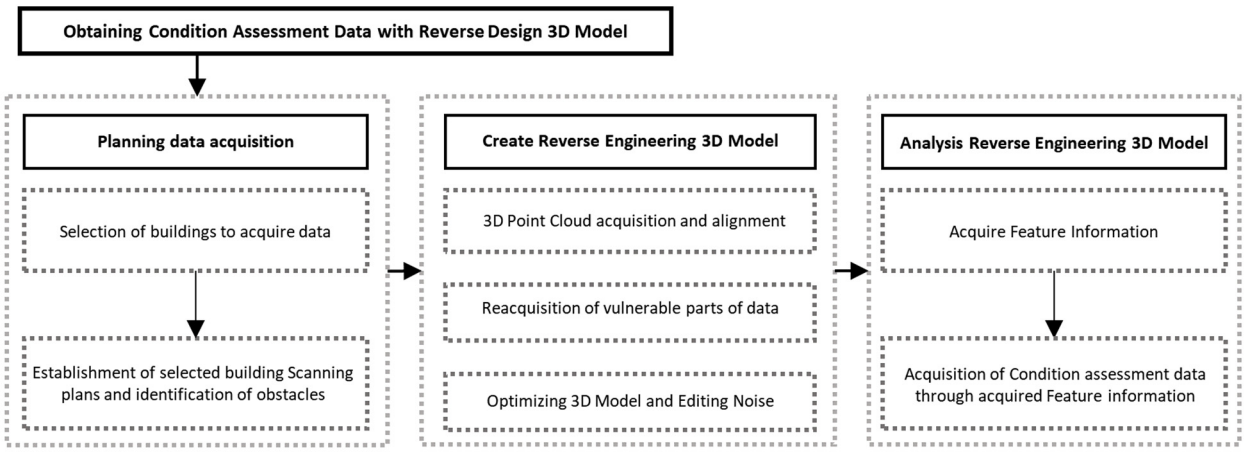

Fig. 3 System architecture of reverse engineering 3D model

Deep-learning training determines the accuracy of the data by dividing the training data, validation data, and test data in a 70:15:15 ratio for automatic learning and validation processes. The DNN structure is optimized to compare the results of the derived data with the actual values to determine the accuracy and reliability of the DNN presented in this study.

3.2 Data acquisition using reverse engineering

3.2.1 Reverse engineering process

Reverse engineering is a technique that uses 3D point cloud data to obtain shape information, and it is essential for building appearance investigation and status diagnosis. Therefore, in this study, a reverse engineering 3D model is generated by using an alignment process to obtain 3D point cloud data with building shape information (Fig. 3).

The target building was a deteriorated three-story building for which a laser scanner (BLK 360) acquired exterior and interior data, and a UAV (Inspire 4) acquired high-floor data. The 3D point cloud data were recorded in a 3D model with shape information through Cyclone (Leica Geosystems, Balgach, Switzerland), and a reverse engineering 3D model was generated with 3DReshaper (Leica). The total number of images shot was 50 from the laser scanner and 231 from the UAV, with a total shooting time of 2 h 50 min. The 3D point cloud registration took 2 h 10 min, and reverse engineering 3D modeling took 1 h. Data acquisition took 3 h 10 min based on the model for status evaluation of seven items and 55 locations. As a result, the total time required for the process proposed in this study was 9 h, an increase of 40% (considering 5 h is required for visual inspection of the same area). However, the time required for visual inspection is for four people (20 h in total). Thus, the process proposed in this study is more productive from time and cost perspectives.

The existing comparison safety diagnosis process consists of nine evaluation items (strength, neutralization, cracks, scaling, spalling and layer separation, water leaks and efflorescence, rebar exposure, slope, and displacement deformation). However, the reverse engineering 3D model has only shape information, making it difficult to grasp physical elements. Therefore, in this study, independent variables for deep learning comprised seven evaluation items other than physical elements (the same seven evaluation items from the comparison process), so results were not affected. Evaluation items and criteria stipulated by the Korea Authority of Land & Infrastructure Safety were adopted (Table 1).

3.2.2 Status evaluation data acquisition method using the reverse engineering 3D model

Reverse engineering 3D model for cracks, scaling, spalling and delamination, leaks and efflorescence, rebar exposure, slope, and displacement deformation (Fig. 4).

1) Cracks

Cracks were observed with the generated reverse engineering 3D model. To determine the results, the distance between the two end points over the width of the cracks was measured and analyzed considering evaluation criteria stipulated by the Korea Authority of Land & Infrastructure Safety. The number of cracks in the target building was 131, and the average crack was 0.101 mm, which is within 0.1 mm <= X < 0.2 mm, which is the standard evaluation for grade B. Therefore, the result from comprehensive evaluation of all cracks in the building was that the status of cracks was grade B.

2) Scaling

The depth values for scaling (sc) were derived by identifying and comparing the x, y, and z values of the points specified in scaled and normal concrete. The average value for peeling in the target building was 0.22 mm, which corresponds to 0 mm < sc < 0.5 mm for the grade B evaluation standard. In addition, since the area ratio was less than 10%, the final evaluation grade was B.

3) Spalling

A value of the spalling depth (sd) is derived by comparing the Z axis of the part peeling off the concrete wall body against the normal Z axis of the concrete. The average depth of spalling in three places was 5.3 mm, which corresponds to 0 mm < sd < 15 mm, which is the standard evaluation for grade B. In addition, since the area ratio was less than 20%, the final evaluation grade was B.

4) Water Leaks & Efflorescence

Status ratings of water leaks and efflorescence are determined based on the area of the building. The boundary of an area is specified by a polyline, and a mesh is created to calculate the area used for measurement. Therefore, the average area of water leakage and white moss in the building was 0.824 m^2. As a result, the area rating of white embryos, which is the standard evaluation for grade B, was less than 5%, so status was confirmed as grade B.

5) Rebar Exposure

Fig. 5 Reverse engineering 3D model-based condition assessment data acquisition process

Four places in this building had exposed reinforcement. The status rating for rebar exposure (ra) is determined in terms of building area, and the average area of reinforcement exposure was 0.0089 m^2. This corresponds to 0% < ra < 1.0% for the B rating, so it was also confirmed as grade B.

6) Slope

The slope of the building is determined from displacement of the most inclined part by comparing the actual BIM model with the actual 3D model of the building as created with reverse engineering technology. Therefore, the slope of the building was measured in six locations, averaging 0.0007587, which is included in the grade A criteria (below 1/1750), and slope was confirmed as grade A.

7) Displacement deformation

Displacement deformation of each slab can be confirmed by overlapping the BIM model and the reverse engineering 3D model based on a 2D drawing. Therefore,

displacement and deformation values for six parts of the building were 0.006 mm, and the evaluation standard for

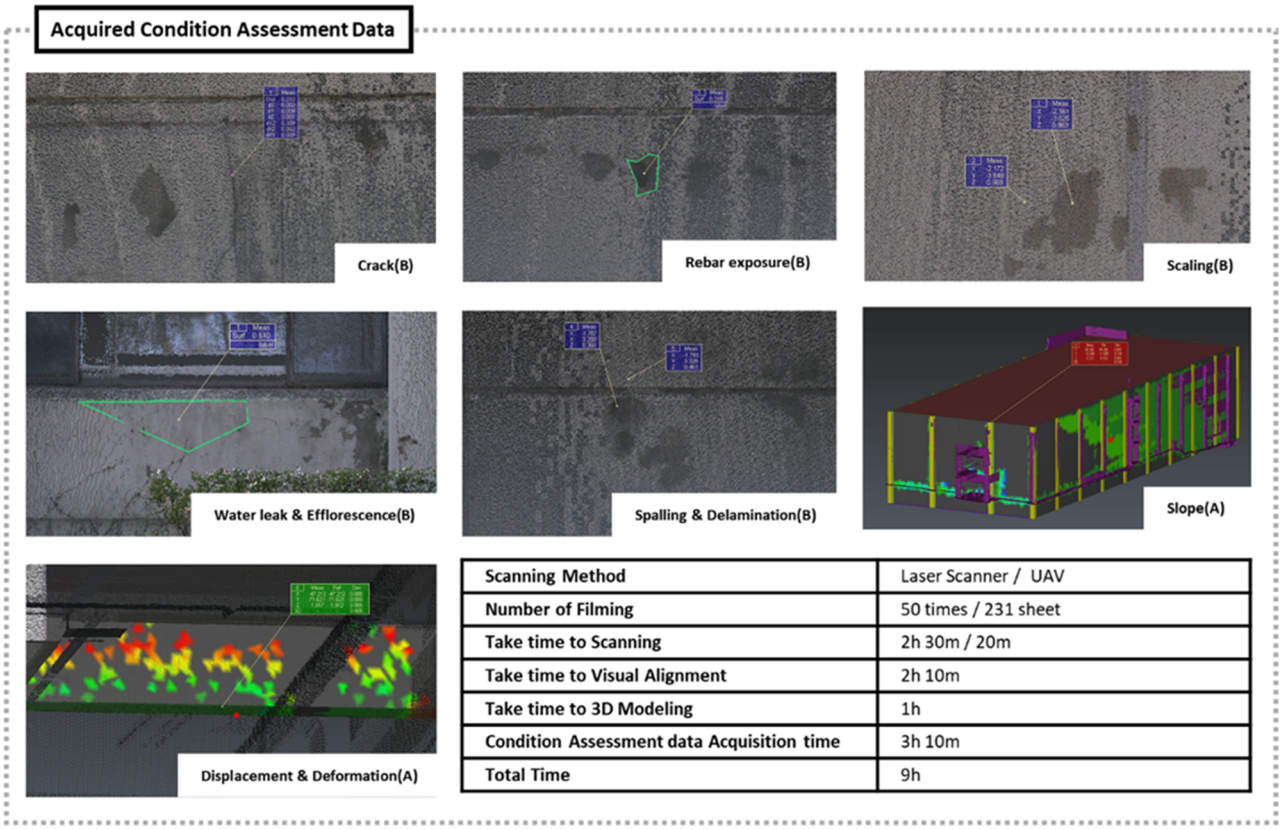

Fig. 4 Acquired condition assessment data

Table 1 Status assessment criteria

	Rating	Score	Criteria		
			Maximum crack width : cw	Area Ratio : 20% or less	Area Ratio : 20% or more
Crack	a	1	cw < 0.1	a	a
	b	3	0.1 <= cw < 0.2	b	c
	c	5	0.2 <= cw < 0.3	c	d
	d	7	0.3 <= cw < 0.5	d	e
	e	9	0.5 <= cw	e	e
	Rating	Score	Criteria		
			Scaling depth : sc	Area Ratio : 10% or less	Area Ratio : 10% or more
Scaling	a	1	Sc = 0	a	a
	b	3	0<= sc <0.5	b	b
	c	5	0.5<= sc <1.0	c	c
	d	7	1.0<= sc <2.5	d	d
	e	9	2.5<= sc	e	e
	Rating	Score	Criteria		
			Spalling and delamination depth : sd	Area Ratio : 20% or less	Area Ratio : 20% or more
Spalling & delamination	a	1	Sd = 0	a	a
	b	3	0<= sd <15	b	c
	c	5	15<= sd <20	c	d
	d	7	20<= sd <25	d	e
	e	9	25<= sd	e	e

Table 1 Continued

	Rating	Score	Criteria		
			Maximum crack width : cw	Area Ratio : 20% or less	Area Ratio : 20% or more
Water leak & efflorescence	Rating	Score	Criteria		
	a	1	No water leak and efflorescence		
	b	3	If there is a trace of minor leakage in a dry state, or the area rate of whitening occurs is less than 5%		
	c	5	Significant signs of water leakage in wet conditions or less than 5% to 10% of white coating occurrence area		
	d	7	he progress of the leak is observable, or the area rate of whitening is less than 10-20%		
	e	9	The progress of leakage is evident, or the area rate of whitening occurs at least 20%		
Rebar exposure	Rating	Score	Criteria		
	a	1	ra = 0		
	b	3	0 < ra < 1.0%		
	c	5	1.0 <= ra < 3.0		
	d	7	3.0 <= ra < 5.0		
	e	9	5.0 <= ra		
Displacement deformation	Rating	Score	Criteria		
	a	1	L (span length) / 480 or less		
	b	3	L / 480 or less		
	c	5	L / 240 or less		
	d	7	L / 150 or less		
	e	9	L / 150 or more		
Slope	Rating	Score	Criteria		
			Slope	Evaluation contents	
	a	1	1/750 or less	Risk subsidence limits on sensitive mechanical foundations.	
	b	3	l/500 or less	Construction Crack Occurrence Limits	
	c	5	1/250 or less	Detect the slope of a structure	
	d	7	1/150 or less	Limits to which structural damage is expected	
	e	9	1/150 or more	To the extent that the structure is dangerous	

grade A is an interim length (L) of 480 or less. Therefore, it was possible to analyze the data intuitively, because it can be visually identified as grade A.

The average error between data acquired from the reverse engineering 3D model and the data acquired from existing visual inspection is in Table 2. The error of each element was sufficiently small to not affect the evaluation grade of the deteriorated building's safety diagnosis.

4. DNN-based deteriorated building safety grade calculation

4.1 Selection of deteriorated buildings, and acquisition of status evaluation data

A case study was conducted on 20 deteriorated buildings that were more than 30 years old. A laser scanner acquired exterior and interior data, and a UAV (Inspire 2) acquired data for high-floor areas. The 20 target buildings had safety grade data calculated from existing visual surveys that could be verified by comparing the results obtained from the safety grade calculation process proposed in this study. The data acquisition method for each building was based on the methods listed in the 3D point cloud data acquisition methodology (Fig. 5). The results of using the acquired 3D point cloud data to analyze the matching reverse engineering 3D model are in Table 3.

4.2 Deep learning–based data training

The DNN proposed in this study consists of an input layer, an output layer, and three hidden layers. If the number of nodes is greater than the number of variables, the learned DNN can suffer from overfitting, so the first hidden layer had three nodes, the second hidden layer had six nodes, and the third hidden layer had five nodes. The training process involved randomly partitioning the dataset of 1000 instances into training, validation, and testing sets. Training was conducted according to the Levenberg-Marquardt algorithm, and performance was evaluated using Mean Squared Error. The training proceeded over 59 epochs, resulting in accuracies surpassing 91% across the entire dataset through linear analysis by the DNN. Specifically, the accuracy on the training set was 91.8%, on the validation set was 92.2%, and on the test set was 91.5%

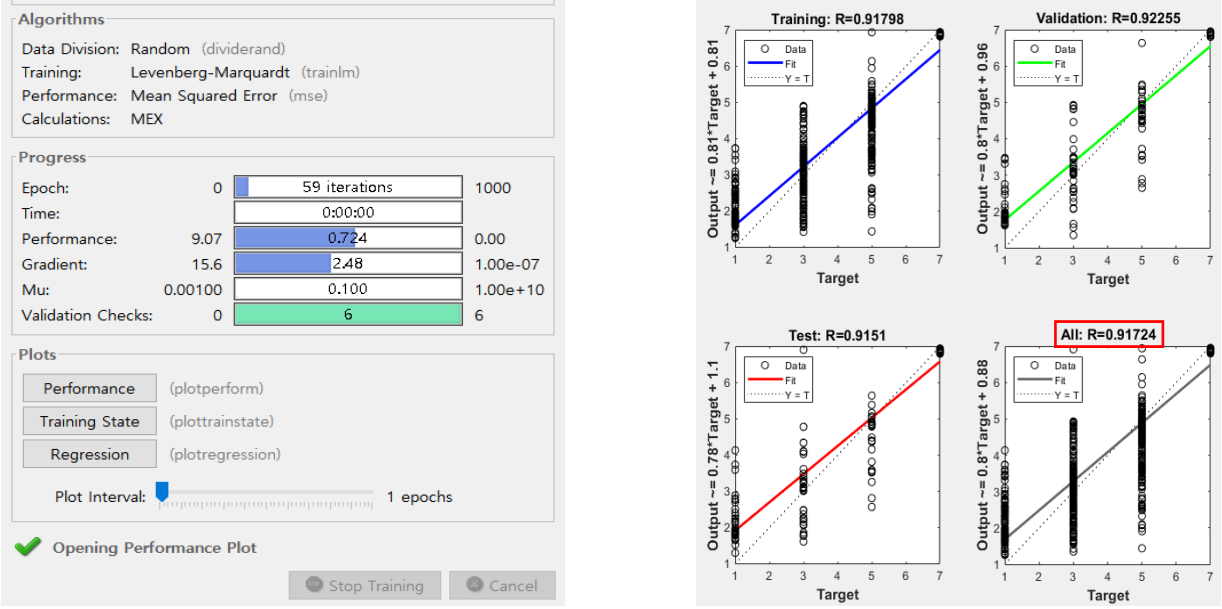

Fig. 6 Learned DNN neural network learning results

Table 2 Average value of error for each element

Element	Crack	Scaling	Spalling & delamination	Water leak & efflorescence	Rebar exposure	Displacement deformation	Slope
Average error	0.101 mm	0.22 mm	5.3 mm	0.824 m^2	0.0089 m^2	0.006	0.0007587
State assessment	No change	No change	No change	No change	No change	No change	No change

Table 3 Acquired condition assessment data

Building	**No. 1**	**No. 2**	**No. 3**	**No. 4**	**No. 5**	**No. 6**	**No. 7**	**No. 8**	**No. 9**	**No. 10**
Crack	5	3	3	3	3	5	9	3	3	3
Scaling	1	3	1	3	3	3	1	1	1	1
Spalling & delamination	3	1	1	3	3	3	1	1	3	1
Water leak & efflorescence	1	1	3	3	3	1	3	3	3	3
Rebar exposure	3	1	1	3	3	3	3	1	3	3
Displacement deformation	1	1	1	1	1	1	1	1	1	1
Slope	1	1	1	1	1	1	1	1	1	1
Building	**No. 11**	**No. 12**	**No. 13**	**No. 14**	**No. 15**	**No. 16**	**No. 17**	**No. 18**	**No. 19**	**No. 20**
Crack	3	5	5	5	5	7	9	5	9	9
Scaling	3	1	3	3	5	7	5	3	5	1
Spalling & delamination	3	3	5	3	5	7	5	3	9	9
Water leak & Efflorescence	3	3	5	3	5	5	5	7	3	9
Rebar exposure	3	1	3	3	5	7	5	3	3	9
Displacement deformation	1	1	1	1	1	3	3	5	1	3
Slope	1	1	1	1	1	3	3	5	3	5

Table 4 Error in measurement data and actual data

Building	No. 1	No. 2	No. 3	No. 4	No. 5	No. 6	No. 7	No. 8	No. 9	No. 10
Resulting value	3.683	1.8241	2.6149	1.9	2.6	2.1	4.6	2.6	2.7	3.3
Rating value	B (3)	A (1)	B (3)	A (1)	B (3)	B (3)	C (5)	B (3)	B (3)	B (3)
Actual value	A (1)	A (1)	A (1)	A (1)	B (3)	B (3)	B (3)	B (3)	B (3)	B (3)
Building	**No. 11**	**No. 12**	**No. 13**	**No. 14**	**No. 15**	**No. 16**	**No. 17**	**No. 18**	**No. 19**	**No. 20**
Resulting value	3.0	3.2	2.5	2.5	4.16	4.47	4.61	4.66	6.89	6.94
Rating value	B (3)	B (3)	B (3)	B (3)	C (5)	C (5)	C (5)	C (5)	D (7)	D (7)
Actual value	B (3)	B (3)	B (3)	B (3)	C (5)	C (5)	C (5)	C (5)	D (7)	D (7)

(Fig. 6).

4.3 Comparative analysis of existing and resulting values

The purpose of this study is to verify the accuracy of the safety grade data for 20 buildings obtained through the existing visual investigation and safety diagnosis process, as compared with the safety grade calculation process proposed in this paper. After applying TargetData (the status evaluation value of the building) to the DNN, the comprehensive evaluation result values were derived. In addition, the results were categorized into grades A, B, C, and D, and the accuracy of each grade was verified by comparing them with the existing values (Table 4).

1) Grade A

Comparing the derived values with the existing values, the accuracy seemed to be reduced. However, if the resulting values are integerized according to grade A, about 50% percent of the values will be obtained from grades B, A, B, and A.

2) Grade B

If the derived values are integerized according to the grade B standard, they were about 90% accurate.

3) Grade C

If the derived values are integerized according to grade C criteria, the levels obtained were 100% accurate.

4) Grade D

If the resulting values are applied to the grade D standard and grade D values are calculated, grade D was derived. Therefore, it was 100% accurate.

Comprehensively, a DNN with about 90% accuracy was generated. In the case of grades C and D, the accuracy was high, but errors occurred in terms of accuracy for grades A and B. This is attributed to the reliance on existing values extracted based on subjective judgment. Consequently, the results obtained using DNN were evaluated much more conservatively than the actual grades, particularly yielding grades equal to or lower than the respective grades for A and B.

Overall, errors occurred in the accuracy of the overall grades for the same reasons, but the focus was on using these grade calculations for maintenance decisions such as conservative reinforcement. The grading calculation presented through the proposed methodology yields conservative results, making it safer for utilization in maintenance aspects.

5. Conclusions

The safety rating–calculation process for aging buildings, as proposed in this study, confirmed that objective status evaluation data can be obtained using a UAV and a laser scanner. Therefore, we confirmed that time and costs can be saved by obtaining status evaluation data without using various expensive devices usually used in safety diagnosis.

In this study, the status evaluation data obtained from the reverse engineering 3D model were applied to a trained DNN, and the accuracy of the DNN was verified by comparing the derived values with existing values. The independent variables of the DNN learning and verification data were the same for seven types of data that can be obtained from shape information. Therefore, the accuracy of the learned DNN was about 90%, and although physical data, such as neutralization and strength, were not included, a safety rating for aging buildings can be calculated objectively and accurately.

However, the safety grade calculation process proposed in this study is limited to reinforced concrete buildings. Therefore, in order to be applied to steel and masonry buildings, new variables must be generated and applied in deep learning. In addition, the safety grade calculation process for aging buildings proposed in this study was automated only in certain parts, such as deep learning. In the future, additional components, such as automated state evaluation data calculation, are needed. Therefore, it is necessary to use deep learning and 3D point cloud data to calculate the integration level of buildings, which is expected to improve objectivity and save money and time through faster state evaluation and integrated-level calculation.

Acknowledgments

This work was supported by the 2022 Yeungnam University Research Grant.

References

Ani, A.I.C., Johar, S., Tawil, N.M., Abd Razak, M.Z. and Hamzah, N. (2015), "Building information modeling (BIM)-based building condition assessment: A survey of water ponding defect on a flat roof", *J. Teknol.*, **75**(9), 25-31. https://doi.org/10.11113/jt.v75.5222

Anuar, M.Z.T., Sarbini, N.N., Ibrahim, I.S., Osman, M.H., Ismail, M. and Khun, M.C. (2019), "A comparative of building condition assessment method used in Asia countries: A review", *IOP Conf Ser. Mater. Sci. Eng.*, **513**(1), 012029. https://doi.org/10.1088/1757-899X/513/1/012029

Cha, Y.J., Choi, W. and Büyüköztürk, O. (2017), "Deep learning-based crack damage detection using convolutional neural networks", *Comput.-Aided Civil Infrastr. Eng.*, **32**(5), 361-378. https://doi.org/10.1111/mice.12263

Chaiyasarn, K., Buatik, A., Mohamad, H., Zhou, M., Kongsilp, S., and Poovarodom, N. (2022), "Integrated pixel-level CNN-FCN crack detection via photogrammetric 3D texture mapping of concrete structures", *Automat. Constr.*, **140**, 104388. https://doi.org/10.1016/j.autcon.2022.104388

Chen, Z., Zhang, W., Huang, R., Dong, Z., Chen, C., Jiang, L. and Wang, H. (2022), "3D model-based terrestrial laser scanning (TLS) observation network planning for large-scale building facades", *Automat. Constr.*, **144**, 104594. https://doi.org/10.1016/j.autcon.2022.104594

Cheng, J.C., Chen, W., Chen, K. and Wang, Q. (2020), "Data-driven predictive maintenance planning framework for MEP components based on BIM and IoT using machine learning algorithms", *Automat. Constr.*, **112**, 103087. https://doi.org/10.1016/j.autcon.2020.103087

Choi, J., Yeum, C.M., Dyke, S.J. and Jahanshahi, M.R. (2018), "Computer-aided approach for rapid post-event visual evaluation of a building façade", *Sensors*, **18**(9), 3017. https://doi.org/10.3390/s18093017

El-Abbasy, M.S., Senouci, A., Zayed, T., Mirahadi, F. and Parvizsedghy, L. (2014), "Artificial neural network models for predicting condition of offshore oil and gas pipelines" *Automat. Constr.*, **45**, 50-65. https://doi.org/10.1016/j.autcon.2014.05.003

Ensafi, M. and Thabet, W. (2021), "Challenges and gaps in facility maintenance practices", *EPiC Series Built Environ.*, **2**, 237-245.

Falorca, J.F. and Lanzinha, J.C.G. (2020), "Facade inspections with drones–theoretical analysis and exploratory tests", *Int. J. Build. Pathol. Adapt.* https://doi.org/10.1108/IJBPA-07-2019-0063

Gopalakrishnan, K., Gholami, H., Vidyadharan, A., Choudhary, A. and Agrawal, A. (2018), "Crack damage detection in unmanned aerial vehicle images of civil infrastructure using pre-trained deep learning model", *Int. J. Traffic Transport Eng.*, **8**(1), 1-14. http://dx.doi.org/10.7708/ijtte.2018.8(1).01

Guo, J. and Wang, Q. (2022), "Human-related uncertainty analysis for automation-enabled façade visual inspection: A Delphi study", *J. Manag. Eng.*, **38**(2), 04021088. https://doi.org/10.1061/(ASCE)ME.1943-5479.0001000

Kang, D. and Cha, Y.J. (2018), "Autonomous UAVs for structural health monitoring using deep learning and an ultrasonic beacon system with geo-tagging", *Comput.-Aided Civil Infrastr. Eng.*, **33**(10), 885-902. https://doi.org/10.1111/mice.12375

Kang, T.W., Kim, J.E. and Jung, T.S. (2016), "Study on 3D Reverse Engineering-based MEP Facility Management Improvement Method", *Korea Inst. Constr. Technol.*, **17**(8), 38-45. https://doi.org/10.5762/KAIS.2016.17.8.38

Kim, Y.S. (2020), "Current Status of Old Buildings and Future Tasks", *Nat. Assembly Res. Serv.*, **133**, 1-13.

Klapa, P. (2023), "Integration of terrestrial laser scanning and UAV-based photogrammetry for heritage Building Information Modeling", *Geomatics, Landmanagement and Landscape*. https://doi.org/10.15576/GLL/2023.1.23

Kwan, A.K.H. and Ng, P.L. (2015), "Building diagnostic techniques and building diagnosis: The way forward", In: *Engineering Asset Management-Systems, Professional Practices and Certification*: *Proceedings of the 8th World Congress on Engineering Asset Management* (*WCEAM 2013*) *& the 3rd International Conference on Utility Management & Safety* (*ICUMAS*), pp. 849-862. https://doi.org/10.1007/978-3-319-09507-3_74

Kwon, S.W. (2009), "Object Recognition and Modeling Technology Using Laser Scanning and BIM for Construction Industry", *Rev. Architect. Build. Sci.*, **53**(4), 31-38.

Kwon, N.Y., Song, K.S., Ahn, Y.H., Park, M.S. and Jang, Y.J. (2020), "Maintenance cost prediction for aging residential buildings based on case-based reasoning and genetic algorithm", *J. Build. Eng.*, **28**, 101006. https://doi.org/10.1016/j.jobe.2019.101006

Laefer, D.F., Truong-Hong, L., Carr, H. and Singh, M. (2014), "Crack detection limits in unit based masonry with terrestrial laser scanning", *Ndt & E Int.*, **62**, 66-76. https://doi.org/10.1016/j.ndteint.2013.11.001

Lattanzi, D. and Miller, G.R. (2014), "3D scene reconstruction for robotic bridge inspection", *J. Infrastr. Syst.*, **21**(2). https://doi.org/10.1061/(ASCE)IS.1943-555X.0000229

Law, D.W., Holden, L. and Silcock, D. (2015), "The assessment of crack development in concrete using a terrestrial laser scanner (TLS)", *Austral. J. Civil Eng.*, **13**(1), 22-31. https://doi.org/10.1080/14488353.2015.1092635

Liu, D., Chen, J., Hu, D. and Zhang, Z. (2019), "Dynamic BIM-augmented UAV safety inspection for water diversion project", *Comput. Indust.*, **108**, 163-177. https://doi.org/10.1016/j.compind.2019.03.004

Marcus, G. (2018), "Deep learning: A critical appraisal", Technical Report; Departments of Psychology and Neural Science, New York University, New York, USA. https://doi.org/10.48550/arXiv.1801.00631

Mukupa, W., Roberts, G.W., Hancock, C.M. and Al-Manasir, K. (2016), "A review of the use of terrestrial laser scanning application for change detection and deformation monitoring of structures", *Survey Review*, **49**(353), 99-116. https://doi.org/10.1080/00396265.2015.1133039

Nex, F., Duarte, D., Tonolo, F.G. and Kerle, N. (2019), "Structural building damage detection with deep learning: Assessment of a state-of-the-art CNN in operational conditions", *Remote Sensing*, **11**(23), 2765. https://doi.org/10.3390/rs11232765

Pan, N.H., Tsai, C.H., Chen, K.Y. and Sung, J. (2020), "Enhancement of external wall decoration material for the building in safety inspection method", *J. Civil Eng. Manag.*, **26**(3), 216-226. https://doi.org/10.3846/jcem.2020.11925

Park, J. and Kim, S.G. (2020), "Structural Safety Management for Small-scale Buildings", The Seoul Institute, 1-115.

Park, H.J., Ryu, J.R., Woo, S.H. and Choo, S.Y. (2016), "An improvement of the building safety inspection survey method using laser scanner and BIM-based reverse engineering", *J. Architect. Inst. Korea Plann. Des.*, **32**(12), 79-90. https://doi.org/10.5659/JAIK_PD.2016.32.12.79

Park, H.J., Lee, S.H., Kim, E.J. and Choo, S.Y. (2017), "A proposal for building safety diagnosis processes using bim-based reverse engineering technology", *Proceeding of the 22nd International conference of the Association for Computer-Aided Architectural Design Research in Asia*, pp. 673-683.

Perez, H., Tah, J.H. and Mosavi, A. (2019), "Deep learning for detecting building defects using convolutional neural networks", *Sensors*, **19**(16), 3556. https://doi.org/10.3390/s19163556

Luo, Q., Ge, B. and Tian, Q. (2019), "A fast adaptive crack detection algorithm based on a double-edge extraction operator

of FSM", *Constr*. *Build*. *Mater*., **204**, 244-254. https://doi.org/10.1016/j.conbuildmat.2019.01.150

Rachmawati, T.S.N. and Kim, S. (2022), "Unmanned Aerial Vehicles (UAV) integration with digital technologies toward construction 4.0: A systematic literature review", *Sustainability*, **14**(9), 5708. https://doi.org/10.3390/su14095708

Sarker, M.M., Ali, T.A., Abdelfatah, A., Yehia, S. and Elaksher, A. (2017), "A cost-effective method for crack detection and measurement on concrete surface", *Int*. *Arch*. *Photogramm*. *Remote Sens*. *Spatial Inform*. *Sci*., **42**, 237. https://doi.org/10.5194/isprs-archives-XLII-2-W8-237-2017

Shi, Z. and Ergan, S. (2018), "Leveraging Point Cloud Data Detecting Building Facade Deterioration Caused by Neighboring Consturction", *Tamap J*. *Eng*. https://doi.org/10.29371/2018.3.66

Shi, Z. and Ergan, S. (2020), "Towards Point Cloud and Model-Based Urban Façade Inspection: Challenges in the Urban Façade Inspection Process", In: *Constuction Research Congress 2020* : *Safety*, *Workforce*, *and Education*, pp. 385-394.

Silva, A., Dias, J.L., Gaspar, P.L. and de Brito, J. (2013), "Statistical models applied to service life prediction of rendered façades", *Automat*. *Constr*., **30**, 151-160. https://doi.org/10.1016/j.autcon.2012.11.028

Sousa, V., Matos, J.P. and Matias, N. (2014), "Evaluation of artificial intelligence tool performance and uncertainty for predicting sewer structural condition", *Automat*. *Constr*., **44**, 84-91. https://doi.org/10.1016/j.autcon.2014.04.004

Tsai, Y.C.J. and Li, F. (2012), "Critical assessment of detecting asphalt pavement cracks under different lighting and low intensity contrast conditions using emerging 3D laser technology", *J*. *Transport*. *Eng*., **138**(5), 649-656. https://doi.org/10.1061/(ASCE)TE.1943-5436.0000353

Turkan, Y., Hong, J., Laflamme, S. and Puri, N. (2018), "Adaptive wavelet neural network for terrestrial laser scanner-based crack detection", *Automat*. *Constr*., **94**, 191-202. https://doi.org/10.1016/j.autcon.2018.06.017

Vasić, D., Ninkov, T., Bulatović, V., Sušić, Z. and Marković, M. (2014), "Terrain mapping by applying unmanned aerial vehicle and lidar system for the purpose of designing in Serbia", *FIG*, *Ingeo*, pp. 217-222.

Wu, J., Shi, Y., Wang, H., Wen, Y. and Du, Y. (2023), "Surface Defect Detection of Nanjing City Wall Based on UAV Oblique Photogrammetry and TLS", *Remote Sens*., **15**(8), 2089. https://doi.org/10.3390/rs15082089

Zhang, J., Qian, S. and Tan, C. (2023), "Automated bridge crack detection method based on lightweight vision models", *Complex Intell*. *Syst*., **9**(2), 1639-1652. https://doi.org/10.1007/s40747-022-00876-6